Chemistry Research Journal, 2020, 5(1):32-46

Available online www.chemrj.org

Research Article

ISSN: 2455-8990
CODEN(USA): CRJHA5

A DFT Analysis of the Relationships between Electronic Structure and Human κ, δ and μ Opioid Receptor Binding Affinity in a series of Diphenethylamines

Juan S. Gómez-Jeria[1]*, Carlos Eduardo Soloaga Ardiles[2], Gaston A. Kpotin[3]

[1]Quantum Pharmacology Unit, Department of Chemistry, Faculty of Sciences, University of Chile. Las Palmeras 3425, Santiago 7800003, Chile
[2]Departamento de Química, Universidad de Tarapacá, Av. General Velásquez 1775, P.O. Box 7-D, Arica, Chile
[3]Laboratory of Theoretical Chemistry and Molecular Spectroscopy, Faculty of Sciences and Technique, University of Abomey-Calavi, 03 BP 3409 Cotonou-Benin

Abstract An analysis of the relationships between electronic structure and mu, delta and kappa receptor binding affinity in a set of diphenethylamines was carried our using the Klopman-Peradejordi-Gómez method. Statistically significant results were obtained for the three opioid receptors. An analysis of the results was performed on the basis of the local molecular orbital structure and the local atomic reactivity indices of the atoms appearing in the resulting QSAR equations. Suggestions about the possible nature of each atom-site interaction were presented. With these data we built the 2D pharmacophores that should help to design molecules with higher or lower receptor affinity.

Keywords Klopman-Peradejordi-Gómez model, KPG, Diphenethylamines, κ opioid receptor, δ opioid receptor, μ opioid receptor, DFT, QSAR

Introduction

Opioid receptors are inhibitory G protein-coupled receptors that are widely distributed through the central nervous system [1]. These receptors were present at the origin of jawed vertebrates about 450 million years ago. They are activated by endogenous opioids such as dynorphins, encephalins, endorphins, endomorphins and nociception [1]. In humans they mediate the body's reaction to most hormones, neurotransmitters and some drugs. Also, they are involved in sensory perception of vision, taste and olfaction [2, 3]. The main known types of opioid receptors are named μ (three subtypes), δ (two subtypes) and κ (three subtypes). These structures are involved in a variety of processes such as analgesia, antidepressant, convulsant and anticonvulsant effects, physical dependence, respiratory depression, sedation and miosis. Unhappily, these receptors are also the target of external agents, such us naturally occurring morphine and codeine, and synthetic molecules such as tramadol, fentanyl, oxycodone, hydrocodone and methadone. The use of some of these molecules leads to opiate addiction [4].

Before these molecules exert their biological activity, they must bind to one or more receptors. This process is described quantitatively by the equilibrium constant (or affinity constant). Our Unit has been interested in the relationships between the electronic structure of some of these molecules and their opioid receptor(s) affinity [5-8]. Recently, a group of molecules called diphenethylamines has been synthesized and tested for binding to the opiate receptors or other biological activities [9-12]. The article of Spetea et al. provided a list of a series of

diphenethylamines with their κ, δ and μ opioid receptor affinity. This prompted us to investigate these molecules. Here we present the results of a theoretical analysis of the relationships between the electronic structure and the opioid receptor (μ, δ and κ) affinity of these molecular systems.

Methods, Models and Calculations [13, 14]

The Method

The method of Klopman-Peradejordi-Gómez (KPG) was employed to obtain the structure-affinity relationships. As the model has been extensively presented and reviewed we refer the reader to the literature [15-23]. The KPG method has shown has proven its effectiveness beyond all reasonable doubt [6, 24-40].

Selection of Molecules and Biological Activities

The molecules are a group of diphenethylamines that were selected from a recent study [10]. Their general formula and receptor binding affinities are displayed, respectively, in Fig. 1 and Table 2.

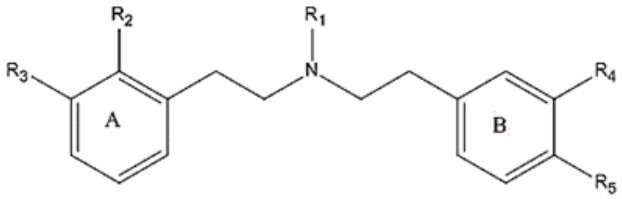

Figure 1: General formulas of diphenethylamines

Table 1: Diphenethylamines and receptor affinities

Mol.	R_1	R_2	R_3	R_4	R_5	log(K_i) KOP	log(K_i) MOP	log(K_i) DOP
1	cyclopentylmethyl	H	OH	H	H	-1.77	2.44	3.35
2	cyclohexylmethyl	H	OH	H	H	-1.21	2.76	3.33
3	benzyl	H	OH	H	H	-0.15	2.67	3.27
4	cyclobutyl	H	OH	H	H	1.01	2.83	3.55
5	isoamyl	H	OH	H	H	0.43	2.41	3.44
6	cyclobutylmethyl	H	OH	OH	H	-0.42	2.36	3.52
7	cyclopropylmethyl	H	OH	OH	H	0.66	2.80	3.45
8	allyl	H	OH	OH	H	0.28	2.55	2.87
9	cyclohexylmethyl	H	OH	OH	H	-0.85	2.22	3.16
10	cyclopentylmethyl	H	OH	OH	H	-0.51	2.77	3.44
12	isoamyl	H	OH	OH	H	0.32	2.32	3.17
12	cyclobutylmethyl	H	OH	H	OH	0.54	1.21	2.63
13	cyclohexylmethyl	H	OH	H	OH	0.27	2.37	3.21
14	allyl	H	OH	H	OH	1.64	2.28	3.04
15	cyclopropylmethyl	H	OH	H	OH	0.55	2.66	----
16	cyclobutylmethyl	F	OH	H	H	-1.14	2.60	----
17	cyclohexylmethyl	F	OH	H	H	-1.40	2.93	----
18	cyclobutylmethyl	F	OH	OH	H	-0.92	2.75	----
19	cyclobutylmethyl	F	OH	H	OH	0.53	2.72	3.12
20	cyclobutylmethyl	H	H	H	H	1.90	3.03	3.34

Table 2 shows the square of the correlation coefficients of the sets of experimental data analyzed here.

Table 2: Correlation between experimental data

	log(K_i) KOP	log(K_i) DOP	log(K_i) MOP
log(K_i) KOP	1.00		
log(K_i) DOP	0.00	1.00	
log(K_i) MOP	0.14	0.07	1.00

We can see that there is a significant correlation between the κ-opioid receptor binding affinity and the functional activity at the same receptor.

Calculations

The electronic structure of all molecules was calculated in the protonated form with the Density Functional Theory (DFT) at the B3LYP/6-31g(d,p) level after full geometry optimization. The Gaussian collection of programs was used[41]. All the information to calculate the numerical values of the local atomic reactivity indices was obtained from the Gaussian results using the D-Cent-QSAR software [42]. All electron populations smaller than or equal to 0.01 e were considered as zero. Negative electron populations coming from Mulliken Population Analysis were corrected as usual [43]. Since the resolution of the system of linear equations is not possible because we have not sufficient molecules, we used Linear Multiple Regression Analysis (LMRA) techniques to find the best solution. For each case, a matrix containing the dependent variable (the receptor affinity of each case) and the local atomic reactivity indices of all atoms of a common skeleton (see below) as independent variables was built. The Statistica software was used for LMRA [44]. We worked within the common skeleton supposition asserting that there is a certain collection of atoms, common to all molecules analyzed, that accounts for approximately all the biological activity. The common skeleton for diphenethylamines is shown in Fig. 2.

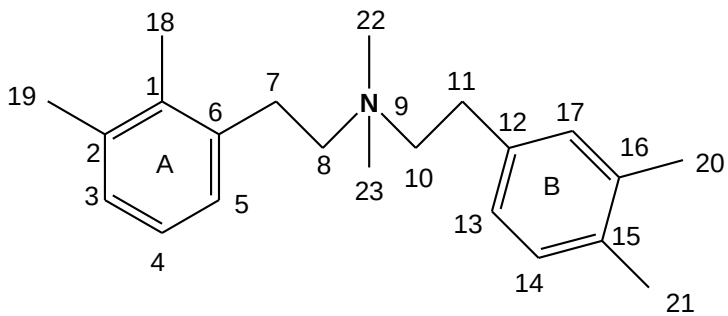

Figure 2: Common skeleton of diphenethylamines

Results

We must mention that the local atomic reactivity indices are not normalized since they have a concrete physical meaning. Therefore the coefficients are not normalized. This is essential for preserving the physics of the equation and also for comparison with other studies carried out with diverse molecules interacting with the same receptors. The KPG method has not the requirement to execute external and internal validations because of its mathematical formal structure. Validation is mandatory for empirical equations of the form "*some biological activity = combination of all indices at hand*" plus any kind of statistical analysis [45]. The analysis of the results was carried out using the procedure recently published [22].

Results for κ-opioid (KOP) receptor affinity

The best equation obtained was:

$$\begin{aligned} log(K_i) &= 3.98 - 3.70Q_{19}^{\max} + 6.13F_{23}(HOMO-2)^* + 0.28S_{12}^N(LUMO)^* \\ &+0.26S_{11}^N(LUMO+2)^* + 0.01S_{21}^N(LUMO+2)^* - \\ &-0.14S_6^N(LUMO+1)^* + 9.11S_8^E(HOMO-1)^* \end{aligned} \quad (1)$$

with n=19, R= 0.98, R^2= 0.96, adj. R^2= 0.94, F (6,12) = 50.12 (p<0.000001) and a standard error of estimate of 0.24. No outliers were detected and no residuals fall outside the ±2σ limits. Here, $Q_{19}^{\max}$ is the maximal amount of charge atom 19 may receive, $F_{23}(HOMO-2)^*$ is the electron population of the third highest occupied MO localized on atom 23, $S_{12}^N(LUMO)^*$ is the nucleophilic superdelocalizability of the lowest empty MO localized on atom 12, $S_{11}^N(LUMO+2)^*$ is the nucleophilic superdelocalizability of the third lowest empty MO localized on atom 12, $S_{21}^N(LUMO+2)^*$ is the nucleophilic superdelocalizability of the third lowest empty MO localized on atom 21,

$S_6^N(LUMO+1)^*$ is the nucleophilic superdelocalizability of the second lowest empty MO localized on atom 6 and $S_8^E(HOMO-1)^*$ is the electrophilic superdelocalizability of the second highest occupied MO localized on atom 8. Tables 3 and 4 show the beta coefficients, the results of the t-test for significance of coefficients and the matrix of squared correlation coefficients for the variables of Eq. 1. There are no significant internal correlations between independent variables (Table 4). Figure 3 displays the plot of observed *vs.* calculated log(K_i).

Table 3: Beta coefficients and t-test for significance of coefficients in Eq. 1

Variable	Beta	t (12)	p-level
$Q_{19}^{\max}$	-0.44	-12.95	< 0.000001
$F_{23}(HOMO-2)^*$	0.57	18.48	< 0.000001
$S_{12}^N(LUMO)^*$	0.46	13.78	< 0.000001
$S_{11}^N(LUMO+2)^*$	0.25	7.58	< 0.000007
$S_{21}^N(LUMO+2)^*$	0.26	8.67	< 0.000002
$S_6^N(LUMO+1)^*$	-0.22	-6.60	< 0.00003
$S_8^E(HOMO-1)^*$	0.20	5.72	< 0.0001

Table 4: Matrix of squared correlation coefficients for the variables in Eq. 1

	$Q_{19}^{\max}$	$F_{23}(HOMO-2)^*$	$S_{12}^N(LUMO)^*$	$S_{11}^N(LUMO+2)^*$	$S_{21}^N(LUMO+2)^*$	$S_6^N(LUMO+1)^*$
$F_{23}(HOMO-2)^*$	0.01	1.00				
$S_{12}^N(LUMO)^*$	0.00	0.08	1.00			
$S_{11}^N(LUMO+2)^*$	0.02	0.01	0.01	1.00		
$S_{21}^N(LUMO+2)^*$	0.02	0.01	0.00	0.02	1.00	
$S_6^N(LUMO+1)^*$	0.13	0.00	0.01	0.02	0.02	1.00
$S_8^E(HOMO-1)^*$	0.06	0.00	0.09	0.15	0.00	0.00

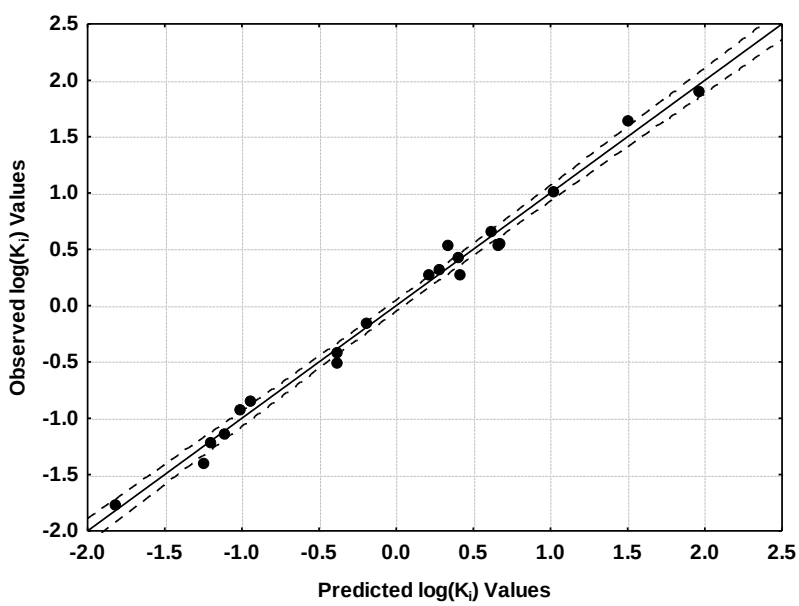

Figure 3: Plot of predicted vs. observed log(K_i) values for the case of κ-opioid receptor affinities (Eq. 1). Dashed lines denote the 95% confidence interval

The associated statistical parameters of Eq. 1 indicate that this equation is statistically significant and that the variation of the numerical values of a group of seven local atomic reactivity indices of atoms of the common

skeleton explains about 94% of the variation of log(K_i) in this group of diphenethylamines. Figure 3, spanning about 4 orders of magnitude, shows that there is a good correlation of observed *versus* calculated values.

Results for μ-opioid (MOP) receptor affinity

The best equation obtained was:

$$log(K_i) = 3.50 - 4.46F_{20}(LUMO+2)^* + 2.09F_{21}(LUMO+2)^* + \\ +0.08S_2^N(LUMO+2)^* - 0.44S_{23}^E(HOMO-2)^* + 0.48S_{19}^E(HOMO)^* \quad (2)$$

with n=19, R= 0.98, R^2= 0.97, adj. R^2= 0.96, F (5,13) = 77.98(p<0.000001) and a standard error of estimate of 0.08. No outliers were detected and no residuals fall outside the ±2σ limits. Here, $F_{20}(LUMO+2)^*$ is the electron population of the third lowest empty MO localized on atom 20, $F_{21}(LUMO+2)^*$ is the electron population of the third lowest empty MO localized on atom 21, $S_2^N(LUMO+2)^*$ is the nucleophilic superdelocalizability of the third lowest empty MO localized on atom 2, $S_{23}^E(HOMO-2)^*$ is the electrophilic superdelocalizability of the third highest occupied MO localized on atom 23 and $S_{19}^E(HOMO)^*$ is the electrophilic superdelocalizability of the highest occupied MO localized on atom 19. Tables 5 and 6 show the beta coefficients, the results of the t-test for significance of coefficients and the matrix of squared correlation coefficients for the variables of Eq. 2. There are no significant internal correlations between independent variables (Table 6). Figure 4 displays the plot of observed *vs.* calculated log(K_i) values.

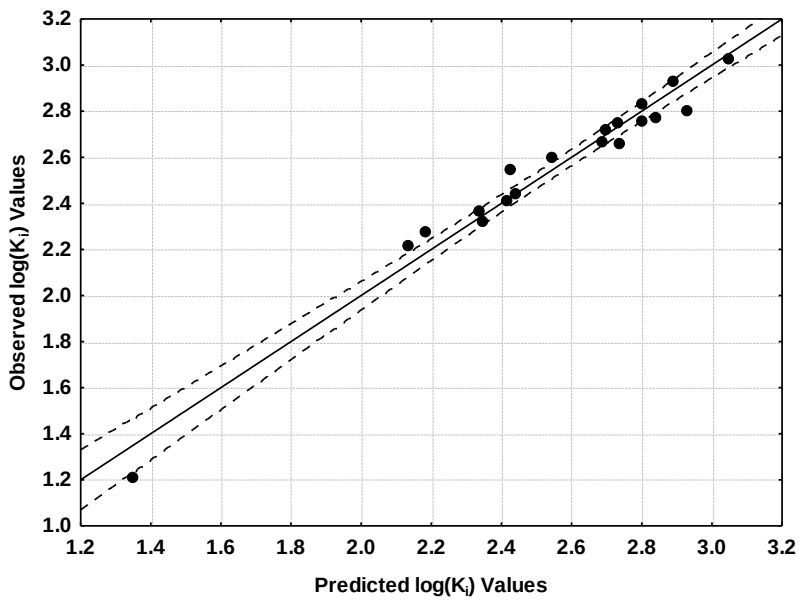

Figure 4: Plot of predicted vs. observed log(K_i) values (Eq. 2). Dashed lines denote the 95% confidence interval

Table 5: Beta coefficients and t-test for significance of coefficients in Eq. 2

Variable	Beta	t (13)	p-level
$F_{20}(LUMO+2)^*$	-0.82	-16.01	< 0.000001
$F_{21}(LUMO+2)^*$	0.28	5.47	< 0.0001
$S_2^N(LUMO+2)^*$	0.45	8.57	< 0.000001
$S_{23}^E(HOMO-2)^*$	-0.22	-4.22	< 0.001
$S_{19}^E(HOMO)^*$	0.45	8.73	< 0.000001

Table 6: Matrix of squared correlation coefficients for the variables in Eq. 2

	$F_{20}(LUMO+2)^*$	$F_{21}(LUMO+2)^*$	$S_2^N(LUMO+2)^*$	$S_{23}^E(HOMO-2)^*$
$F_{21}(LUMO+2)^*$	0.00	1.00		
$S_2^N(LUMO+2)^*$	0.04	0.00	1.00	
$S_{23}^E(HOMO-2)^*$	0.00	0.02	0.05	1.00
$S_{19}^E(HOMO)^*$	0.01	0.00	0.00	0.04

The associated statistical parameters of Eq. 2 indicate that this equation is statistically significant and that the variation of the numerical values of a group of five local atomic reactivity indices of atoms of the common skeleton explains about 96% of the variation of log(K_i) values.Figure 4, spanning about 2 orders of magnitude, shows that there is a good correlation of observed *versus* calculated values.

Results for δ-opioid (DOP) receptor affinity

The best equation obtained was:

$$log(K_i) = 1.74 - 0.30\mu_{14}^* + 0.25S_{19}^E(HOMO-2)^* - 1.65F_8(LUMO)^* - 0.21F_5(HOMO-1)^* \quad (3)$$

with n=15, R= 0.98, R^2= 0.97, adj. R^2= 0.96, F (4,10) = 76.56 (p<0.000001) and a standard error of estimate of 0.04. No outliers were detected and no residuals fall outside the ±2σ limits. Here, μ_{14}^* is the local atomic electronic chemical potential of atom 14, $S_{19}^E(HOMO-2)^*$ is the electrophilic superdelocalizability of the third highest occupied MO localized on atom 19, $F_8(LUMO)^*$ is the electron population of the lowest empty MO localized on atom 8 and $F_5(HOMO-1)^*$ is the electron population of the second highest occupied MO localized on atom 5.Tables 7 and 8 show the beta coefficients, the results of the t-test for significance of coefficients and the matrix of squared correlation coefficients for the variables of Eq. 3. There are no significant internal correlations between independent variables (Table 8). Figure 3 displays the plot of observed *vs.* calculated log(K_i).

Table 7: Beta coefficients and t-test for significance of coefficients in Eq. 3

Variable	Beta	t (10)	p-level
μ_{14}	-0.46	-7.09	< 0.00003
$S_{19}^E(HOMO-2)^*$	0.60	9.76	< 0.000002
$F_8(LUMO)^*$	-0.25	-4.28	< 0.002
$F_5(HOMO-1)^*$	-0.19	-3.09	< 0.01

Table 8: Matrix of squared correlation coefficients for the variables in Eq. 3

	μ_{14}	$S_{19}^E(HOMO-2)^*$	$F_8(LUMO)^*$
$S_{19}^E(HOMO-2)^*$	0.14	1.00	
$F_8(LUMO)^*$	0.01	0.02	1.00
$F_5(HOMO-1)^*$	0.15	0.04	0.00

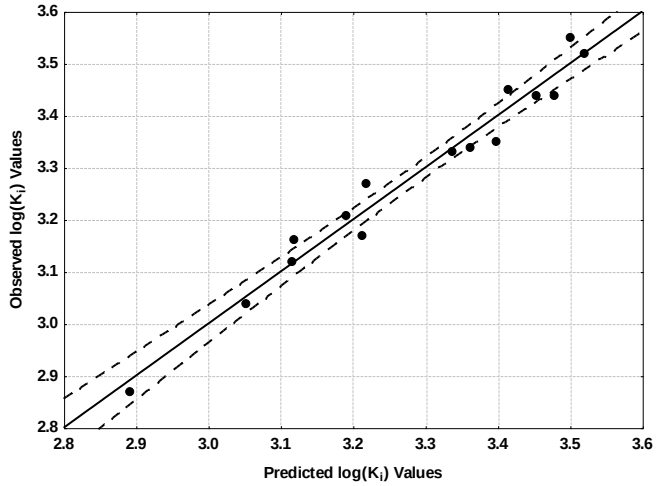

Figure 5: Plot of predicted vs. observed log(K_i) values (Eq. 3). Dashed lines denote the 95% confidence interval

The associated statistical parameters of Eq. 3 indicate that this equation is statistically significant and that the variation of the numerical values of a group of four local atomic reactivity indices of atoms of the common skeleton explains about 96% of the variation of log(K_i). Figure 5, spanning about 0.6 orders of magnitude, shows that there is a good correlation of observed *versus* calculated values and that almost all points are inside or close to the 95% confidence interval.

Local Molecular Orbitals

Tables 9 to 13 show the local MO structure of atoms 2, 5, 6, 8, 9, 10, 11, 12, 14 and 18-23 (see Fig. 2). Nomenclature of the Tables: Molecule (HOMO number) / (HOMO-2)* (HOMO-1)* (HOMO)* - (LUMO)* (LUMO+1)* (LUMO+2)*. The reader must note that when a local atomic reactivity index of an inner occupied MO (i.e., HOMO-1 and/or HOMO-2) or of a higher vacant MO (LUMO+1 and/or LUMO+2) appears inside and equation, this means that the remaining of the upper occupied MOs (for example, if HOMO-2 appears in an equation, upper means HOMO-1 and HOMO) or the remaining empty MOs (for example, if LUMO+1 appears, lower means the LUMO) also contribute to the interaction. Their absence in the equation only means that the variation of their numerical values does not account for the variation of the numerical value of the biological property.

Table 9: Local Molecular orbitals of atoms 2, 5 and 6

Molecule	Atom 2	Atom 5	Atom 6
1 (88)	82σ83π88π-91π93π100σ	83π8788π-91π93π94σ	83π87π88π-90π91π92σ
2 (92)	83σ85π92π-93π94π95π	85π86π92π-93π94π95π	86σ89π92π-93π95σ96π
3 (85)	76σ77π85π-88π89π90π	78π82π85π-88π89π90π	77π82π85π-88π89π90π
4 (80)	75σ76π80π-83π84π90σ	76π79π80π-83π84π86σ	76π79π80π-82π83π84π
5 (85)	79σ80σ85π-88π89π91π	80σ81π85π-88π89π90π	83π84π85π-88π89π90π
6 (88)	81σ84π88π-90π93π96σ	84π86π88π-90π93π107π	84π86π88π-90π91π92σ
7 (84)	74σ77σ84π-87π88π95π	79π82π84π-87π88π107σ	80σ82π84π-86π87π88π
8 (80)	73σ74π79π-83π84π85π	73σ74π79π-82π83π84π	74π77π79π-82π83π85π
9 (96)	86σ87π95π-97π98π99π	86σ87π95π-97π98π99π	87π93π95π-97π99π100π
10 (92)	81σ82π91π-93π94π95π	84π85π91π-93π94π95π	85π89π91π-93π94σ95π
11 (89)	79σ80π88π-90π91π92π	80π86π88π-90π91π92π	80σ86π88π-90π91π92π
12 (88)	78σ79π87π-89π90π91π	82π85π87π-89π91π93π	82π85π87π-89π91π 93π
13 (96)	88σ89π96π-98π99π101π	89π94π96π-98π99π101π	89π94π96π-98σ99σ100σ
14 (80)	72σ74π79π-82π85π86π	74π75π79π-82π85π86π	77π78π79π-82σ85σ86σ
15 (84)	75σ76π83π-85π86π87π	78π81π83π-85π86π87π	78π81π83π-85π86π87π
16 (88)	78σ79π88π-89π92π93π	80σ81π88π-89π92π93σ	81π85π88-89π90π92π

17 (96)	84σ93π96π-97π98π99π	84σ93π96π-97π98π99π	87π93π96π-97π101π103π
18 (92)	81σ82σ91π-93π94π95π	83π85σ91π-93π94π95π	83π89π91π-93π94π95π
19 (92)	82σ91π92π-94π95π96π	85π91π92π-94π95σ96π	85π90π91π-93π94π95π
20 (80)	77π79π80π-81π82π83π	77π79π80π-81π82π83π	78π79π80π-81π82π83π

Table 10: Local Molecular orbitals of atoms 8, 9 and 10

Molecule	Atom 8	Atom 9	Atom 10
1 (88)	75σ83σ87σ-91σ92σ93σ	75σ80σ82σ-91σ94σ95σ	75σ77σ86σ-89σ92σ94σ
2 (92)	83σ85σ89σ-93σ96σ97σ	79σ80σ85σ-98σ99σ101σ	80σ83σ91σ-94σ96σ97σ
3 (85)	76σ77σ82σ-86σ87σ88σ	77σ78σ80σ-86σ90σ93σ	78σ80σ84σ-86σ89σ90σ
4 (80)	75σ76σ79σ-83σ85σ86σ	70σ73σ74σ-86σ87σ88σ	73σ74σ78σ-81σ82σ85σ
5 (85)	80σ81σ84σ-88σ89σ90σ	71σ72σ73σ-91σ92σ93σ	73σ75σ83σ-86σ87σ90σ
6 (88)	75σ84σ86σ-89σ90σ91σ	75σ79σ82σ-90σ96σ97σ	78σ80σ85σ-89σ91σ92σ
7 (84)	79σ80σ82σ-87σ88σ89σ	69σ79σ80σ-87σ91σ92σ	75σ76σ81σ-85σ86σ89σ
8 (80)	69σ74σ77σ-81σ82σ83σ	67σ71σ76σ-82σ83σ88σ	75σ76σ7σ-81σ82σ83σ
9 (96)	86σ87σ93σ-97σ100σ102σ	79σ80σ91σ-98σ102σ103σ	84σ89σ94σ-97σ98σ100σ
10 (92)	82σ87σ89σ-93σ94σ95σ	79σ84σ86σ-98σ99σ101σ	84σ87σ90σ-94σ95σ97σ
11 (89)	79σ80σ86σ-90σ91σ94σ	80σ82σ83σ-95σ96σ97σ	82σ85σ87σ-91σ94σ95σ
12 (88)	79σ81σ85σ-89σ93σ95σ	76σ81σ82σ-94σ95σ96σ	81σ82σ88σ-91σ92σ93σ
13 (96)	85σ89σ94σ-99σ100σ101σ	80σ83σ84σ-98σ103σ104σ	84σ87σ95σ- 99σ100σ102σ
14 (80)	72σ74σ78σ-81σ82σ84σ	69σ71σ76σ-81σ82σ85σ	71σ75σ80σ-81σ84σ87σ
15 (84)	76σ80σ81σ-85σ86σ87σ	74σ79σ80σ-90σ92σ93σ	77σ78σ84σ-88σ89σ90σ
16 (88)	79σ81σ85σ-89σ90σ92σ	77σ82σ83σ-94σ96σ97σ	79σ80σ87σ-90σ93σ94σ
17 (96)	84σ87σ93σ-97σ101σ103σ	83σ86σ88σ-99σ102σ104σ	85σ86σ95σ-98σ99σ101σ
18 (92)	82σ83σ89σ-93σ96σ97σ	77σ79σ86σ-100σ101σ102σ	85σ86σ90-94σ95σ97σ
19 (92)	81σ85σ90σ-93σ94σ95σ	82σ87σ88σ-94σ98σ99σ	86σ87σ92σ-95σ96σ98σ
20 (80)	68σ69σ79σ-82σ85σ86σ	66σ70σ72σ-81σ86σ87σ	68σ69σ80σ-81σ82σ85σ

Table 11: Local Molecular orbitals of atoms 11, 12 and 14

Molecule	Atom 11	Atom 12	Atom 14
1 (88)	77σ78σ86σ-89σ99σ101σ	78σ85π86π-89π90π91π	78σ85π86π-89π90π92π
2 (92)	83σ84σ91σ-94σ100σ102σ	84σ90π91π-94π95π96π	84σ90π91π-94π95π96π
3 (85)	78σ79σ84σ-90σ92σ96σ	78σ79σ84π-89π90π91π	79σ83π84π-89π90π91π
4 (80)	72σ73σ78σ-81σ87σ88σ	72σ77π78π-81π82π86π	73σ77π78π-81π82π83π
5 (85)	75σ76σ83σ-86σ87σ90σ	82π83π84π-86π87π90π	82π83π84π-86π87π90σ
6 (88)	78σ80σ85σ-89σ98σ99	83π85π87π-89π91π92π	83π85π87π-89π91π105π
7 (84)	75σ76σ81σ-85σ86σ91σ	76π81π83π-85π86π89π	76π81π83π-85π86π87π
8 (80)	73σ75σ78σ-82σ83σ84σ	75π78π80π-82π83π84π	75π78π80π-82π83π84π
9 (96)	88σ89σ94σ-98σ101σ103σ	89π94π96π-98π99π100σ	89π94π96π-98π99π101π
10 (92)	84σ87σ90σ-94σ99σ105σ	88π90π92π-94π95π96π	87π90π92π-93π94π95π
11 (89)	81σ82σ87σ-91σ100σ101σ	85π87π89π-90π91π93π	85π87π89π-90π91π92π
12 (88)	81σ82σ88σ-90σ92σ96σ	83π84π88π-90π92π93π	84π86π88π-90π92π105π
13 (96)	86σ87σ95σ-97σ98σ99σ	86σ87π95π-97π98π99π	87π93π95π-97π100π106σ
14 (80)	71σ75σ80σ-84σ85σ86σ	74π75π80π-83π84π85π	77π78π80π-83π84π91π
15 (84)	77σ78σ84σ-85σ88σ91σ	77π78π84π-88π89π90σ	78π82π84π-85π86π87π
16 (88)	80σ81σ87σ-90σ91σ95σ	81σ86π87π-90π91π92π	81σ86π87π-89π90π91π
17 (96)	88σ89σ95σ-99σ101σ105σ	88σ89σ95π-98π99π100π	89σ94π95π-99π100π114π
18 (92)	85σ86σ90σ-94σ96σ101σ	88π90π92π-94π95π96π	88π90π92π-94π95π96π
19 (92)	83σ86σ92σ-93σ95σ96σ	86π91π92π-93π95π96π	89π91π92π-93π94π96π
20 (80)	74σ75σ80σ-82σ85σ87σ	76σ79π80π-81π82π84π	76σ78σ80π-81π82π83π

Table 12: Local Molecular orbitals of atoms 18, 19 and 20

Molecule	Atom 18	Atom 19	Atom 20
1 (88)	70σ76σ82σ-94σ97σ99σ	82σ83π88π-93σ116π135π	65σ77σ78σ-101σ102σ103σ
2 (92)	71σ82σ83σ-97σ98σ99σ	85π86π92π-94π95π96π	69σ83σ84σ-105σ106σ108σ
3 (85)	64σ74σ76σ-92σ93σ94σ	77π78π85π-89π90π101π	69σ78σ79σ-96σ100σ101σ
4 (80)	69σ70σ75σ-86σ87σ88σ	75σ76π80π-84π98π106π	59σ71σ72σ-92σ93σ95σ
5 (85)	71σ79σ80σ-91σ93σ96σ	80σ81π85π-89π105σ126π	75σ76σ77σ-94σ99σ100σ
6 (88)	71σ77σ81σ-95σ96σ98σ	82π84π88π-93π107σ114π	82π83π87π-91π92π106σ
7 (84)	67σ74σ77σ-90σ91σ92σ	79π80π84π-88π110σ126σ	75σ76π83π-86π103σ115π
8 (80)	68σ69σ72σ-87σ88σ90σ	74π75π79π-85π104π108σ	74π75π80π-84π86π106π
9 (96)	74σ79σ86σ-102σ103σ104σ	86σ87π95π-99π113π126π	89π91π96π-101π121π147π
10 (92)	73σ80σ81σ-97σ98σ99σ	85π86π91π-95π113σ115σ	87π88π92π-96π108σ120π
11 (89)	68σ76σ79σ-94σ95σ96σ	80π82π88π-92π105π109π	84π85π89π-93π103σ136σ
12 (88)	83σ84σ88σ-90σ92σ93σ	81π82π87π-91π112σ130σ	65σ76σ80σ-99σ101σ105σ
13 (96)	75σ85σ88σ-102σ105σ107σ	88σ89π96σ-101σ146σ147σ	73σ78σ86σ-109σ110σ111σ
14 (80)	64σ68σ72σ-87σ89σ95σ	74σ75π79π-85π86π97π	70σ71σ73σ-92σ94σ96σ
15 (84)	68σ73σ75σ-89σ90σ91σ	77π78π83π-87π98σ105π	76σ77σ78σ-98σ99σ100σ
16 (88)	81π85π88π-89π92π94π	80π81π88π-89π92π106σ	79σ80σ81σ-99σ101σ102σ
17 (96)	87π93π96π-97π98π103π	87π93π96π-97π98π109π	76σ88σ89σ-108σ110σ113σ
18 (92)	83π89π91π-93π95π98π	85π89π91π-94π95π108π	86π88π92π-96π111π123π
19 (92)	90π91π92π-94π97π99π	85π91π92π-97π116π119σ	82σ91π92π-94π95π96π
20 (80)	71σ73σ74σ-87σ90σ93σ	73σ74σ75σ-93σ94σ95σ	73σ74σ75σ-94σ96σ97σ

Table 13: Local Molecular orbitals of atoms 21, 22 and 23

Molecule	Atom 21	Atom 22	Atom 23
1 (88)	69σ75σ77σ-101σ102σ103σ	61σ62σ68σ-89σ90σ91σ	79σ80σ81σ-89σ92σ94σ
2 (92)	73σ82σ83σ-105σ106σ109σ	66σ69σ89σ-94σ95σ96σ	79σ80σ87σ-94σ97σ98σ
3 (85)	69σ70σ78σ-96σ100σ101σ	64σ77σ85σ-88σ89σ92σ	73σ80σ81σ- 86σ87σ92σ
4 (80)	63σ65σ71σ-92σ93σ94σ	62σ63σ78σ-81σ85σ86σ	73σ74σ76σ-86σ87σ88σ
5 (85)	66σ69σ75σ-94σ97σ98σ	57σ59σ60σ-86σ87σ90σ	80σ81σ84σ-86σ89σ90σ
6 (88)	68σ73σ78σ-98σ100σ101σ	68σ73σ78σ-98σ100σ101	79σ8083σ-89σ91σ92σ
7 (84)	67σ70σ75σ-92σ98σ100σ	68σ69σ81σ-86σ89σ90σ	69σ79σ80σ-87σ89σ91σ
8 (80)	70σ71σ73σ-93σ94σ96σ	53σ58σ60σ-81σ82σ84σ	65σ67σ76σ-81σ88σ89σ
9 (96)	78σ81σ88σ-110σ112σ113σ	63σ65σ70σ-97σ98σ99σ	84σ87σ91σ-97σ99σ100σ
10 (92)	76σ83σ84σ-106σ107σ108σ	66σ67σ89σ-93σ94σ95σ	84σ86σ87σ-97σ99σ101σ
11 (89)	71σ74σ81σ-101σ103σ104σ	68σ80σ88σ-90σ91σ92σ	77σ82σ83σ-94σ95σ96σ
12 (88)	83π84π88π-92π105σ113π	63σ79σ87σ-89σ91σ92σ	82σ83σ84σ-92σ93σ96σ
13 (96)	86π87π95π-98π99π100π	65σ70σ73σ-98σ99σ100σ	87σ90σ91σ-99σ100σ102σ
14 (80)	74π75π80π-84π86π96σ	49σ58σ60σ-81σ82σ84σ	66σ67σ76σ-81σ86σ88σ
15 (84)	78π80π84π-88π99σ109π	64σ69σ83σ-85σ86σ89σ	69σ79σ80σ-89σ91σ92σ
16 (88)	79σ80σ81σ-99σ101σ102σ	64σ67σ85σ-89σ90σ91σ	82σ83σ84σ-93σ94σ95σ
17 (96)	72σ76σ88σ-105σ110σ111σ	69σ71σ93σ-97σ98σ101σ	86σ90σ92σ-101σ103σ104σ
18 (92)	78σ84σ85σ-104σ106σ107σ	65σ66σ70σ-93σ94σ97σ	85σ87σ88σ-96σ97σ98σ
19 (92)	87π91π92π-95π96π107σ	65σ66σ75σ-94σ95σ96σ	86σ87σ88σ-95σ96σ98σ
20 (80)	64σ71σ72σ-94σ96σ97σ	51σ58σ70σ-81σ82σ84σ	74σ75σ76σ-81σ82σ85σ

Discussion

Discussion of the results for kappa opioid (KOP) receptor affinity

Table 3 shows that the importance of variables in Eq. 1 is $F_{23}(HOMO-2)^* > S_{12}^N(LUMO)^* \sim Q_{19}^{\max} > S_{21}^N(LUMO+2)^* \sim S_{11}^N(LUMO+2)^* \sim S_6^N(LUMO+1)^* \sim S_8^E(HOMO-1)^*$. A high kappa receptor binding affinity is associated with positive values for $Q_{19}^{\max}$, small values for $F_{23}(HOMO-2)^*$, small (positive) values for

$S_{12}^{N}(LUMO)^{*}$, small (positive) values for $S_{11}^{N}(LUMO+2)^{*}$, small (positive) values for $S_{21}^{N}(LUMO+2)^{*}$, large (positive) values for $S_{6}^{N}(LUMO+1)^{*}$ and large (negative) values for $S_{8}^{E}(HOMO-1)^{*}$. Atom 19 is the first atom of the substituent attached to atom 1 (H or OH, Fig. 2). Positive values for $Q_{19}^{\max}$ suggest that an atom able to receive extra charge is suitable for a higher receptor affinity. Perhaps a fluorine atom at this position should be studied. Atom 23 is the first atom of the substituent attached to atom 9 (Fig. 2). All MOs have σ nature (Table 13). Atom 23 is a carbon in all cases. The local $HOMO_{23}^{*}$ is energetically far from the molecular HOMO. As small values for $F_{23}(HOMO-2)^{*}$ are associated with high receptor affinity we may infer that small values for $F_{23}(HOMO-1)^{*}$ and $F_{23}(HOMO)^{*}$ are also required for high affinity. We suggest that this atom is interacting with an electron-rich center, perhaps via σ-σ interactions. Atom 12 is a carbon atom belonging to ring B (Fig. 2). Small values for $S_{12}^{N}(LUMO)^{*}$ are associated with high affinity. These values are obtained by increasing the value of the corresponding eigenvalue making this atom a bad electron acceptor. $(LUMO)_{12}^{*}$is a π MO in all cases (Table 11). $(HOMO)_{12}^{*}$ is also a π MO in all cases (Table 11). Therefore, it is suggested that atom 12 is interacting with an electron-deficient center (π-cation or π-π interactions).Atom 11 is a sp^3 carbon atom belonging to the chain linking rings A and B (Fig. 2). All MOs have σ nature (Table 11). High receptor affinity is associated with small (positive) values for $S_{11}^{N}(LUMO+2)^{*}$, making this MO a bad electron acceptor. We hypothesized that the same restriction holds for $S_{11}^{N}(LUMO+1)^{*}$ and $S_{11}^{N}(LUMO)^{*}$. We suggest that this atom is interacting with an alkyl chain of the site (alkyl interaction) through its occupied sigma MOs. Atom 21 is the first atom of the substituent attached to atom 15 (H or OH in ring B, Fig, 2). Small (positive) values for $S_{21}^{N}(LUMO+2)^{*}$ are associated with high receptor affinity. These values are obtained by increasing the value of the corresponding eigenvalue making this atom a bad electron acceptor. Table 13 shows that $(LUMO+2)_{21}^{*}$ has σ or π nature. $(LUMO+1)_{21}^{*}$ and $(LUMO)_{21}^{*}$ also have σ or π nature. The requirement of empty MOs with almost insignificant reactivity allows us to suggest that this atom is interacting with an electron-deficient center. Atom 6 is a carbon atom belonging to ring A (Fig. 2). A high receptor affinity is associated with high (positive) values for $S_{6}^{N}(LUMO+1)^{*}$.

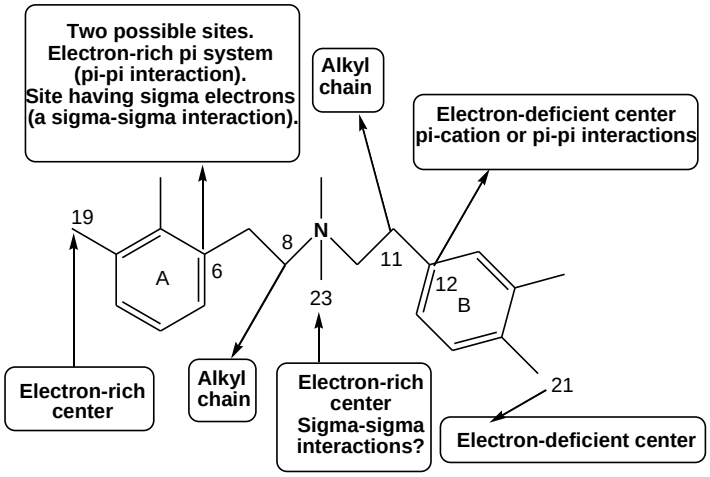

Figure 6: Partial 2D pharmacophore for κ opioid receptor affinity

These values are obtained by diminishing the value of $(LUMO+1)_{6}^{*}$ energy, augmenting the electron-acceptor capacity of this MO. Also, $(LUMO)_{6}^{*}$ energy will diminish. This suggests that these two MOs are interacting with an electron-rich site. On the other hand, Table 9 shows that $(LUMO)_{6}^{*}$ and $(LUMO+1)_{6}^{*}$ may have σ or π nature. This suggests that atom 6 could be interacting with an electron-rich π system (a π-π interaction) and maybe with a site having σ electrons (a σ-σ interaction). Atom 8 is a sp3carbonatom belonging to the chain linking rings A and B (Fig. 2). All MOs have σ nature (Table 10). Large (negative) values for $S_{8}^{E}(HOMO-1)^{*}$ are associated with high

receptor affinity. These values are obtained by shifting the MO energy toward zero making it more reactive. Therefore, atom 8 seems to interact with an alkyl chain situated on the binding site (alkyl interaction). All the suggestions are displayed in the partial 2D pharmacophore of Fig. 6.

Discussion of the results for μ opioid (MOP) receptor affinity

Table 5 shows that the importance of variables in Eq. 2 is $F_{20}(LUMO+2)^* >> S_2^N(LUMO+2)^* = S_{19}^E(HOMO)^*$ $>> F_{21}(LUMO+2)^* > S_{23}^E(HOMO-2)^*$. A high mu receptor binding affinity is associated with large values of $F_{20}(LUMO+2)^*$, small (positive) values of $F_{21}(LUMO+2)^*$ and $S_2^N(LUMO+2)^*$, small (negative) values of $S_{23}^E(HOMO-2)^*$ and large (negative) values of $S_{19}^E(HOMO)^*$. Atom 20 is the atom of the substituent directly attached at position 16 (H or OH, Fig. 2). High μ receptor binding affinities are associated with large values of $F_{20}(LUMO+2)^*$. These values are obtained by raising the electron population of this MO (note that raising the electron population of this MO at this atom diminishes its localization over other atoms, and that the ideal situation would be a MO localized only on this atom), making it more reactive. Table 14 shows that all MOs have a σ nature. Therefore, we suggest that atom 20 could be interacting with an alkyl chain. Atom 21 is the atom of the substituent attached at position 15 (H or OH, Fig. 2). Table 13 shows that all MOs have a σ nature. A high binding affinity is associated with small values of $F_{21}(LUMO+2)^*$. These values are obtained by diminishing the electron population, making this MO less reactive. If this condition also holds for $(LUMO+1)_{21}^*$ and $(LUMO)_{21}^*$, then this atom could also be interacting with an alkyl chain in the binding site. Atom 2 is a carbon in ring A (Fig. 2). A high μ receptor affinity is associated with small (positive) values of $S_2^N(LUMO+2)^*$. Table 9 shows that $(LUMO+2)_2^*$ can have a π or σ nature. $(LUMO+1)_2^*$ and $(LUMO)_2^*$ have a π nature. If the condition for $S_2^N(LUMO+2)^*$ hold also for $S_2^N(LUMO+1)^*$ and $S_2^N(LUMO)^*$, then we suggest that atom 2 is interacting with an electron-deficient π system of the site (or maybe with a cation). Atom 23 is the atom of the substituent attached at position 9 (Fig. 2). Atom 23 is a carbon in all cases. A high binding affinity is associated with small (negative) values of $S_{23}^E(HOMO-2)^*$. Table 13 shows that all local MOs have a σ nature. Small negative values for this index are obtained by raising the MO energy, making it less reactive. Note that only in some cases $(HOMO)_{23}^*$ is energetically very far from the molecular HOMO and that also only in some cases $(LUMO)_{23}^*$ is energetically very far from the molecular LUMO. Now, if the condition for $S_{23}^E(HOMO-2)^*$ also holds for $S_{23}^E(HOMO-1)^*$ and $S_{23}^E(HOMO)^*$ then atom 23 seems to interact with an alkyl chain in the binding site. Atom 19 is the atom of the substituent attached at position 2 (H or OH, Fig. 2). A high binding affinity is associated with large (negative) values of $S_{19}^E(HOMO)^*$. Table 12 shows that $(HOMO)_{19}^*$ has a π nature in all but two cases. Large negative values are obtained mainly by shifting the $(HOMO)_{19}^*$ energy toward zero, making it more reactive.

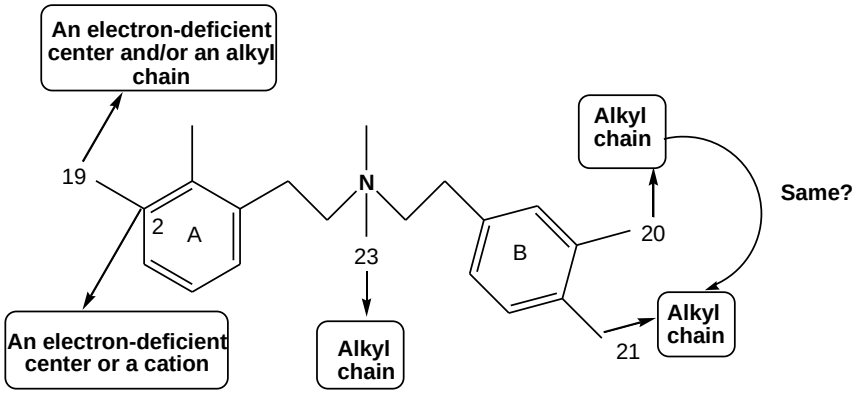

Figure 7: Partial 2D pharmacophore for μ opioid receptor affinity

But Table 12 shows that is some cases $(HOMO)_{19}^{*}$ coincides with the molecular HOMO. In this case the only way to get these values is by raising the electron population of this MO. Now, when $(HOMO)_{19}^{*}$ does not coincide with the molecular HOMO we can substitute the molecule in such a way that the molecular HOMO will be partially localized on atom 19. This suggests that this atom is interacting with an electron-deficient π moiety and/or with an alkyl chain (π-π and/or alkyl interactions).All the suggestions are displayed in the partial 2D pharmacophore of Fig. 7.

Discussion of the results for δ-opioid (DOP) receptor affinity

Table 7 shows that the importance of variables in Eq. 3 is $S_{19}^{E}(HOMO-2)^{*} > \mu_{14} >> F_{8}(LUMO)^{*} > F_{5}(HOMO-1)^{*}$. A high delta receptor binding affinity is associated with small (negative) values for μ_{14}^{*}, large (negative) values for $S_{19}^{E}(HOMO-2)^{*}$ and small values for $F_{8}(LUMO)^{*}$ and $F_{5}(HOMO-1)^{*}$. Atom 19 is the atom of the substituent attached to atom 2 (H or OH, Fig. 2). A high receptor affinity is associated with large (negative) values of S_{19}^{E}(HOMO-2)*. Table 12 shows that the three highest occupied local MOs have π or σ nature. Large (negative) values for this reactivity index are obtained by shifting the $(HOMO\text{-}2)_{19}^{*}$ energy toward zero making this MO more reactive. This process will also make more reactive $(HOMO\text{-}1)_{19}^{*}$ and $(HOMO)_{19}^{*}$. This suggests that atom 19 atom is interacting with an electron-deficient π moiety and/or with an alkyl chain (π-π and/or alkyl interactions).Atom 14 is a carbon in ring B (Fig. 2). A high receptor affinity is associated with small values for μ_{14}^{*}. This reactivity index corresponds to the midpoint between $(HOMO)_{14}^{*}$ and $(LUMO)_{14}^{*}$ and it is usually a negative number. Table 11 shows that in some cases $(HOMO)_{14}^{*}$ coincides with the molecular HOMO. Here, the only way to obtain small negative values for this reactivity index is to shift upwards the energy of $(LUMO)_{14}^{*}$ making it less reactive. This situation suggests that atom 14 is behaving as a π electron-rich center. On the other hand, if $(HOMO)_{14}^{*}$ does not coincide with the molecular HOMO, the small negative values are obtained by shifting upwards the energy of $(HOMO)_{14}^{*}$, i.e. by inserting substituents of the correct nature and in the correct place to oblige the molecular HOMO to localize (partially) on atom 14. The interpretation is the same than the previous case. Therefore, we suggest that atom 14 is engaged in π-cation, π-π, π-σ and/or π-alkyl interactions.Atom 8 is a sp^3 carbon localized in the chain linking rings A and B (Fig. 2).Table 10 shows that all local MOs have a σ nature. A high receptor affinity is associated with small values for F_8(LUMO)*. These values are obtained by substituting the molecule in such a way that this local empty OM be replaced by another molecular MO with a higher energy, making it less reactive. Therefore we suggest that atom 8 is engaged in an alkyl interaction with an alkyl chain of the binding site. Atom 5 is a carbon in ring A (Fig. 2).

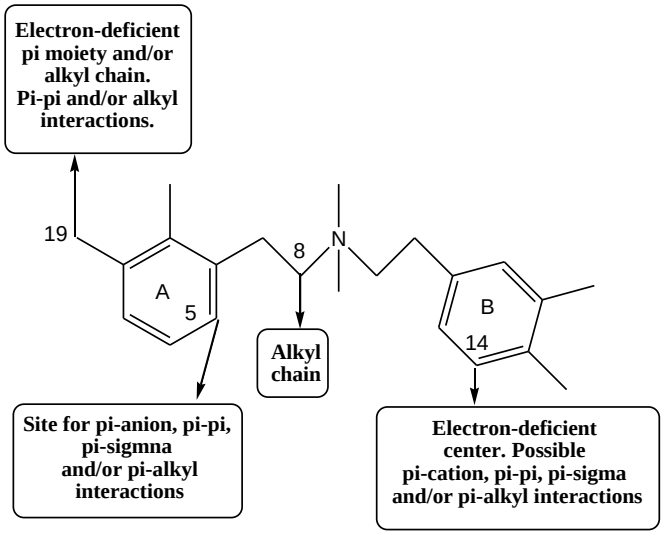

Figure 8: Partial 2D pharmacophore for δ-opioid receptor affinity

Table 9 shows that $(HOMO)_4^*$ has a π nature in all molecules and that $(HOMO\text{-}1)_4^*$ has π or σ natures. $(LUMO)_4^*$ has a π nature. A high receptor affinity is associated with small values for F_5 (HOMO-1)*. These values are obtained by diminishing the electron population of this MO. In the limit situation, the molecular orbital ceases to be localized on that atom. Is this same requirement holds for $(HOMO)_4^*$, then atom 5 is behaving as an electron-deficient center. If this is the case, then this atom seems to be engaged in π-anion, π-π, π-σ and/or π-alkyl interactions. All the suggestions are displayed in the partial 2D pharmacophore of Fig. 8.

In summary, we have obtained statistically significant results showing for each receptor that there is a relationship between the variation of the receptor affinity and the variation of the numerical values of a definite set of local atomic reactivity indices (LARIs). The analysis of the LARIs allowed us to suggest the kind of interactions involved in the drug-receptor interaction. These results are encompassed in the 2D pharmacophore that should be helpful in the design of new molecules endowed with higher or lower receptor affinity and also having more selectivity for only one receptor.

References

[1]. Callaghan, C. K.; Rouine, J.; O'Mara, S. M. Chapter 3 - Potential roles for opioid receptors in motivation and major depressive disorder. In *Progress in Brain Research*, O'Mara, S., Ed. Elsevier: 2018; Vol. 239, pp 89-119.

[2]. Valentino, R. J.; Volkow, N. D. Untangling the complexity of opioid receptor function. *Neuropsychopharmacology* 2018, 43, 2514-2520.

[3]. Stein, C. Opioid Receptors. *Annual Review of Medicine* 2016, 67, 433-451.

[4]. Wang, S. Historical Review: Opiate Addiction and Opioid Receptors. *Cell transplantation* 2019, 28, 233-238.

[5]. Bruna-Larenas, T.; Gómez-Jeria, J. S. A DFT and Semiempirical Model-Based Study of Opioid Receptor Affinity and Selectivity in a Group of Molecules with a Morphine Structural Core. *International Journal of Medicinal Chemistry* 2012, 2012 Article ID 682495, 1-16.

[6]. Gómez-Jeria, J. S.; Gerli-Candia, L. A.; Hurtado, S. M. A structure-affinity study of the opioid binding of some 3-substituted morphinans. *Journal of the Chilean Chemical Society* 2004, 49, 307-312.

[7]. Gómez-Jeria, J. S.; Lagos-Arancibia, L.; Sobarzo-Sánchez, E. Theoretical study of the opioid receptor selectivity of some 7-arylidenenaltrexones. *Boletin de la Sociedad Chilena de Quimica* 2003, 48, 61-66.

[8]. Gómez-Jeria, J. S.; Sotomayor, P. Quantum chemical study of electronic structure and receptor binding in opiates. *Journal of Molecular Structure: THEOCHEM* 1988, 166, 493-498.

[9]. Spetea, M.; Eans, S. O.; Ganno, M. L.; Lantero, A.; Mairegger, M.; Toll, L.; Schmidhammer, H.; McLaughlin, J. P. Selective κ receptor partial agonist HS666 produces potent antinociception without inducing aversion after i.c.v. administration in mice. *British Journal of Pharmacology* 2017, 174, 2444-2456.

[10]. Erli, F.; Guerrieri, E.; Ben Haddou, T.; Lantero, A.; Mairegger, M.; Schmidhammer, H.; Spetea, M. Highly Potent and Selective New Diphenethylamines Interacting with the κ-Opioid Receptor: Synthesis, Pharmacology, and Structure–Activity Relationships. *Journal of Medicinal Chemistry* 2017, 60, 7579-7590.

[11]. Guerrieri, E.; Bermudez, M.; Wolber, G.; Berzetei-Gurske, I. P.; Schmidhammer, H.; Spetea, M. Structural determinants of diphenethylamines for interaction with the κ opioid receptor: Synthesis, pharmacology and molecular modeling studies. *Bioorganic & Medicinal Chemistry Letters* 2016, 26, 4769-4774.

[12]. Spetea, M.; Berzetei-Gurske, I. P.; Guerrieri, E.; Schmidhammer, H. Discovery and Pharmacological Evaluation of a Diphenethylamine Derivative (HS665), a Highly Potent and Selective κ Opioid Receptor Agonist. *Journal of Medicinal Chemistry* 2012, 55, 10302-10306.

[13]. The results presented here are obtained from what is now a routinary procedure. For this reason, we built a general model for the paper's structure. This model contains *standard* phrases for the presentation of the

methods, calculations and results because they do not need to be rewritten repeatedly and the number of possible variations to use is finite.

[14]. All papers of J.S. G.-J. can be found in https://www.researchgate.net/profile/Juan-Sebastian_Gomez-Jeria.

[15]. Gómez-Jeria, J. S.; Ojeda-Vergara, M. Parametrization of the orientational effects in the drug-receptor interaction. *Journal of the Chilean Chemical Society* 2003, 48, 119-124.

[16]. Gómez-Jeria, J. S. Modeling the Drug-Receptor Interaction in Quantum Pharmacology. In *Molecules in Physics, Chemistry, and Biology*, Maruani, J., Ed. Springer Netherlands: 1989; Vol. 4, pp 215-231.

[17]. Gómez-Jeria, J. S. On some problems in quantum pharmacology I. The partition functions. *International Journal of Quantum Chemistry* 1983, 23, 1969-1972.

[18]. Gómez-Jeria, J. S. A New Set of Local Reactivity Indices within the Hartree-Fock-Roothaan and Density Functional Theory Frameworks. *Canadian Chemical Transactions* 2013, 1, 25-55.

[19]. Gómez-Jeria, J. S. *Elements of Molecular Electronic Pharmacology (in Spanish)*. 1st ed.; Ediciones Sokar: Santiago de Chile, 2013; p 104.

[20]. Alarcón, D. A.; Gatica-Díaz, F.; Gómez-Jeria, J. S. Modeling the relationships between molecular structure and inhibition of virus-induced cytopathic efects. Anti-HIV and anti-H1N1 (Influenza) activities as examples. *Journal of the Chilean Chemical Society* 2013, 58, 1651-1659.

[21]. Barahona-Urbina, C.; Nuñez-Gonzalez, S.; Gómez-Jeria, J. S. Model-based quantum-chemical study of the uptake of some polychlorinated pollutant compounds by Zucchini subspecies. *Journal of the Chilean Chemical Society* 2012, 57, 1497-1503.

[22]. Gómez-Jeria, J. S.; Kpotin, G. Some Remarks on The Interpretation of The Local Atomic Reactivity Indices Within the Klopman-Peradejordi-Gómez (KPG) Method. I. Theoretical Analysis. *Research Journal of Pharmaceutical, Biological and Chemical Sciences* 2018, 9, 550-561.

[23]. Gómez-Jeria, J. S. 45 Years of the KPG Method: A Tribute to Federico Peradejordi. *Journal of Computational Methods in Molecular Design* 2017, 7, 17-37.

[24]. Gómez-Jeria, J. S.; González-Ponce, N. A Quantum-chemical study of the relationships between electronic structure and affinities for the serotonin transporter protein and the 5-HT1A receptor in a series of 2H-pyrido[1,2-c]pyrimidine derivatives. *Chemistry Research Journal* 2020, in press.

[25]. Kpotin, G. A.; Bédé, A. L.; Houngue-Kpota, A.; Anatovi, W.; Kuevi, U. A.; Atohoun, G. S.; Mensah, J.-B.; Gómez-Jeria, J. S.; Badawi, M. Relationship between electronic structures and antiplasmodial activities of xanthone derivatives: a 2D-QSAR approach. *Structural Chemistry* 2019, 30, 2301-2310.

[26]. Gómez-Jeria, J. S.; Gatica-Díaz, N. A preliminary quantum chemical analysis of the relationships between electronic structure and 5-HT_{1A} and 5-HT_{2A} receptor affinity in a series of 8-acetyl-7-hydroxy-4-methylcoumarin derivatives. *Chemistry Research Journal* 2019, 4, 85-100.

[27]. Gómez-Jeria, J. S.; Garrido-Sáez, N. A DFT analysis of the relationships between electronic structure and affinity for dopamine D_2, D_3 and D_4 receptor subtypes in a group of 77-LH-28-1 derivatives. *Chemistry Research Journal* 2019, 4, 30-42.

[28]. Kpotin, G.; Gómez-Jeria, J. S. A Quantum-chemical Study of the Relationships Between Electronic Structure and Anti-proliferative Activity of Quinoxaline Derivatives on the HeLa Cell Line. *International Journal of Computational and Theoretical Chemistry* 2017, 5, 59-68.

[29]. Gómez-Jeria, J. S.; Moreno-Rojas, C. A theoretical study of the inhibition of human 4-hydroxyphenylpyruvate dioxygenase by a series of pyrazalone-quinazolone hybrids. *Der Pharma Chemica* 2016, 8, 475-482.

[30]. Gómez-Jeria, J. S.; Robles-Navarro, A. DFT and Docking Studies of the Relationships between Electronic Structure and 5-HT_{2A} Receptor Binding Affinity in N-Benzylphenethylamines. *Research Journal of Pharmaceutical, Biological and Chemical Sciences* 2015, 6, 1811-1841.

[31]. Muñoz-Gacitúa, D.; Gómez-Jeria, J. S. Quantum-chemical study of the relationships between electronic structure and anti influenza activity. 2. The inhibition by 1H-1,2,3-triazole-4-carboxamide derivatives of

the cytopathic effects produced by the influenza A/WSN/33 (H1N1) and A/HK/8/68 (H3N2) strains in MDCK cells. *Journal of Computational Methods in Molecular Design* 2014, 4, 48-63.

[32]. Muñoz-Gacitúa, D.; Gómez-Jeria, J. S. Quantum-chemical study of the relationships between electronic structure and anti influenza activity. 1. The inhibition of cytophatic effects produced by the influenza A/Guangdong Luohu/219/2006 (H1N1) strain in MDCK cells by substituted bisaryl amide compounds. *Journal of Computational Methods in Molecular Design* 2014, 4, 33-47.

[33]. Gómez-Jeria, J. S. Toward Understanding the Inhibition of Vesicular Stomatitis Virus Replication in MDCK Cells by 4-Quinolinecarboxylic acid Analogues. A Density Functional Study. *Der Pharma Chemica* 2014, 6, 64-77.

[34]. Gatica-Díaz, F.; Gómez-Jeria, J. S. A Theoretical Study of the Relationships between Electronic Structure and Cytotoxicity of a group of N^2-alkylated Quaternary β-Carbolines against nine Tumoral Cell Lines. *Journal of Computational Methods in Molecular Design* 2014, 4, 79-120.

[35]. Gómez-Jeria, J. S.; Flores-Catalán, M. Quantum-chemical modeling of the relationships between molecular structure and in vitro multi-step, multimechanistic drug effects. HIV-1 replication inhibition and inhibition of cell proliferation as examples. *Canadian Chemical Transactions* 2013, 1, 215-237.

[36]. Gómez-Jeria, J. S.; Soto-Morales, F.; Rivas, J.; Sotomayor, A. A theoretical structure-affinity relationship study of some cannabinoid derivatives. *Journal of the Chilean Chemical Society* 2008, 53, 1393-1399.

[37]. Gómez-Jeria, J. S.; Lagos-Arancibia, L. Quantum-chemical structure-affinity studies on kynurenic acid derivatives as Gly/NMDA receptor ligands. *International Journal of Quantum Chemistry* 1999, 71, 505-511.

[38]. Gómez-Jeria, J. S.; Ojeda-Vergara, M.; Donoso-Espinoza, C. Quantum-chemical Structure-Activity Relationships in carbamate insecticides. *Molecular Engineering* 1995, 5, 391-401.

[39]. Gómez-Jeria, J. S.; Morales-Lagos, D. R. Quantum chemical approach to the relationship between molecular structure and serotonin receptor binding affinity. *Journal of Pharmaceutical Sciences* 1984, 73, 1725-1728.

[40]. Gómez-Jeria, J. S.; Espinoza, L. Quantum-chemical studies on acetylcholinesterasa inhibition. I. Carbamates. *Journal of the Chilean Chemical Society* 1982, 27, 142-144.

[41]. Frisch, M. J.; Trucks, G. W.; Schlegel, H. B.; Scuseria, G. E.; Robb, M. A.; Cheeseman, J. R.; Montgomery, J., J.A.; Vreven, T.; Kudin, K. N.; Burant, J. C.; Millam, J. M.; Iyengar, S. S.; Tomasi, J.; Barone, V.; Mennucci, B.; Cossi, M.; Scalmani, G.; Rega, N. *G03 Rev. E.01*, Gaussian: Pittsburgh, PA, USA, 2007.

[42]. Gómez-Jeria, J. S. *D-Cent-QSAR: A program to generate Local Atomic Reactivity Indices from Gaussian 03 log files. v. 1.0*, v. 1.0; Santiago, Chile, 2014.

[43]. Gómez-Jeria, J. S. An empirical way to correct some drawbacks of Mulliken Population Analysis (Erratum in: J. Chil. Chem. Soc., 55, 4, IX, 2010). *Journal of the Chilean Chemical Society* 2009, 54, 482-485.

[44]. Statsoft. *Statistica v. 8.0*, 2300 East 14 th St. Tulsa, OK 74104, USA, 1984-2007.

[45]. Martin, Y. C. *Quantitative drug design: a critical introduction*. M. Dekker: New York, 1978; 425 p.